Biochimica et Biophysica Acta 1778 (2008) 1483-1492

Contents lists available at ScienceDirect

Biochimica et Biophysica Acta

journal homepage: www.elsevier.com/locate/bbamem

Membrane partitioning of various δ-opioid receptor forms before and after agonist activations: The effect of cholesterol

Aurore André, Gérald Gaibelet, Laurent Le Guyader, Michèle Welby, André Lopez *, Chantal Lebrun *

IPBS, MR5089 CNRS/UPS, 205 Route de Narbonne, 31077 Toulouse Cedex 4, France

ARTICLE INFO

Article history:
Received 8 January 2008
Received in revised form 10 March 2008
Accepted 24 March 2008
Available online 1 April 2008

Keywords:
GPCR
hDOR
Lateral organization
Raft
Hydrophobic mismatch
Cholesterol

ABSTRACT

Lipid rafts depicted as densely packed and thicker membrane microdomains, based on the dynamic clustering of cholesterol and sphingolipids, may help as platforms involved in a wide variety of cellular processes. The reasons why proteins segregate into rafts are yet to be clarified. The human delta opioid receptor (hDOR) reconstituted in a model system has been characterised after ligand binding by an elongation of its transmembrane part, inducing rearrangement of its lipid microenvironment [Alves, Salamon, Hruby, and Tollin (2005) Biochemistry 44, 9168–9178]. We used hDOR to understand better the correlation between its function and its membrane microdomain localisation. A fusion protein of hDOR with the Green Fluorescent Protein (DOR*) allows precise receptor membrane quantification. Here we report that (i) a fraction of the total receptor pool requires cholesterol for binding activity, (ii) G-proteins stabilize a high affinity state conformation which does not seem modulated by cholesterol. In relation to its distribution, and (iii) a fraction of DOR* is constitutively associated with detergent-resistant membranes (DRM) characterised by an enrichment in lipids and proteins raft markers. (iv) An increase in the quantity of DOR* was observed upon agonist addition. (v) This DRM relocation is prevented by uncoupling the receptor–G-protein interaction.

1. Introduction

Almost 20 years ago, the selective lateral confinement of lipids and proteins to discrete regions in the cell plasma membrane was conceived as functional lipid microdomains, crucial to the function of various biological processes [1]. Indeed, these microdomains probably provide dynamic fluid platforms that segregate membrane components and serve to localise the requisite components with a high concentration, allowing the specificity and the efficiency of responsiveness [2,3]. Thus, direct information relating to the lipid and protein composition of these microdomains, and the identification and characterisation of the driving forces involved in their sorting are subjects of intense investigation [1,4].

The ability of lipids to exist in several phases, including gel, liquid-ordered (*lo*) and liquid-disordered states (*ld*), and to promote particular lipid segregation in a lipid mixture was revealed by model membrane studies. However, rapid lateral exchanges of lipids within this bilayer has been reported [5,6]. *lo* is characterised by tight acyl-chain packing, correlated with extended acyl-chains and a high degree of acyl-chain order, allowing greater hydrophobic thickness than the average thickness of the lipid mixture. *lo* is observed if high concentrations of cholesterol (>30% mol/mol) are mixed with phospholipids (PL) that possess saturated fatty acyl-chains [7]. Cholesterol preferentially interacts with these PL and consequently promotes *lo*/*ld* phase separation in particular lipid mixtures. Sphingomyelin strengthens these domain formations, due to its acylation and its hydrogen bonding with cholesterol [8].

The question of whether lipid rafts, depicted as small platforms in the *lo* state, exist in the plasma membrane of eukaryotic cells has received much attention over the last few years [9,10]. Indeed, cellular plasma membranes are characterised by a relatively high cholesterol content. They are also characterised by the presence of sphingolipids, especially glycosphingolipid, which differ from most biological phospholipids as they contain long, largely saturated acyl-chains. The most compelling piece of evidence for the existence of rafts is based on the observation that a subset of membrane components is resistant to solubilisation with non-ionic detergents at low temperatures. As expected, the purified detergent-resistant membrane fractions (DRMs) are enriched in saturated lipids, sphingomyelin and cholesterol [11] even if the conditions of solubilisation depend strongly on the class of detergent, on the starting material (whole cells or isolated membranes) [12–14] and on the detergent to membrane lipid ratio [15].

The raft regions are also believed to be selective in the membrane protein lateral distributions. Indeed, biochemical analysis of the protein content of DRMs, isolated from several cell types, show a striking concentration of membrane proteins modified by saturated chain lipids, such as Thy-1 (GPI-anchored), LAT (dual palmitoylated) and Lck (myristoylated and palmitoylated), and α subunits of the heterotrimeric G-proteins. They appear to be targeted to rafts, as a result of post-translational modification with saturated lipids [2,16].

* Corresponding authors. Tel.: +33 561175946; fax: +33 561175476.
E-mail addresses: andre.lopez@ipbs.fr (A. Lopez), chantal.lebrun@ipbs.fr (C. Lebrun).

0005-2736/$ – see front matter.
doi:10.1016/j.bbamem.2008.03.017

Rafts may contribute to the regulation of membrane function, and thus the membrane partitioning of proteins, including signalling molecules, has been extensively studied [3,17]. Generally, association with DRMs was used as a criterion for estimating whether a protein associates with lipid rafts, but how this is achieved and the specific effects of selected lipid components remain unclear.

In this study, we focused on hDOR. This receptor appears to be a good candidate for analysing its partitioning in plasma membrane. Studies on reconstituted hDOR in planar-supported bilayers have shown that binding of an agonist to hDOR induces an elongation of the transmembrane hydrophobic part of the receptor and a rearrangement of the surrounding lipid microenvironment [18–20]. These studies suggest that hydrophobic matching between the receptor and the lipid is a driving force for receptor trafficking.

Rafts are characterised by being thicker than the surrounding liquid-disordered regions; thus, we analysed the importance of rafts in hDOR activity expressed in an HEK cell line (i) by measuring the influence of membrane cholesterol content on ligand and G-protein binding, and (ii) by analysing hDOR partitioning in various extracted membranes and its redistribution upon ligand binding. The use of a fusion protein of hDOR with a Green Fluorescent Protein (DOR*) allowed a precise receptor membrane quantification [21]. We show, by modulating the cholesterol content in the membrane, using Methyl-β-cyclodextrin (MβCD), that a fraction of DOR* requires cholesterol for activity. DRMs were then isolated and characterised by solubilisation with cold Triton X-100 (TX-100) using various TX-100 concentrations [14]. Our data show that a fraction of DOR* appears unsolubilised by cold TX-100. We estimated the amount of receptors constitutively associated with the DRMs subset and upon ligand binding. Finally, we discussed whether the observed DOR* regulation by cholesterol was dependent on its localisation in rafts.

2. Materials and methods

2.1. Chemicals

[^{3}H]Diprenorphine (DPN) (50 Ci/mmol) and [^{3}H]Deltorphin II (Del2) (45 Ci/mmol) were purchased from Perkin-Elmer Life Sciences. [^{35}S]-GTPγS (1 mCi/mmol) was purchased from Amersham Biosciences. Non-radioactive ligands, DPDPE ([D-Pen2,D-Pen5]-Enkephalin), were purchased from Sigma-Aldrich. Scintillation fluid (Ready protein$^+$) was purchased from Beckman Coulter. MβCD and cholesterol (Chol) were purchased from Sigma-Aldrich. Lipid standard (Avanti Polar Lipid) and sterol purity was checked by TLC (Kiesegel 60 CF254, Merck). We purchased 1-Myristoyl-2-[12-[(7-nitro-2-1,3-benzoxadiazol-4-yl)amino]dodecanoyl]-*sn*-Glycero-3-Phosphate (NBD-PA) from Avanti Polar Lipids. Dimethylformamide (DMF) was purchased from SDS. Salts and solvents were of analytical grade.

2.2. Construction of the recombinant eGFP-tagged hDOR, DNA transfections and cell culture

A recombinant human embryonic kidney cell line (HEK 293), expressing stable hDOR fused to a T7 tag sequence at the N-terminus and to eGFP at the C-terminus, was prepared and used in this study. pcDNA plasmids encoding hDOR was a generous gift from Dr. B. L. Kieffer (University Louis Pasteur, Illkirch, France). First, recombinant hDOR lacking the ATG codon was amplified by PCR, using the 5′-CACGTGTACGTAGAACCGGCCCCCTCCGCCGGC-3′ sense and the 5′-GTCTAGATTAGCTAGCGGCGGCAGCGCCACCGCCGGG-3′ antisense primers. These primers contained an SnaBI site (underlined) at the 5′ end of the sense primer and NheI site (underlined) at the 5′ end of the antisense primer. Second, the amplified fragment (1.1 Kb) digested by SnaBI and NheI was inserted into the SmaI and NheI sites of the bluescsript SK+ plasmid containing the construct SP/α7AChR-T7-eGFP-hMOR [22], in which the hMOR fragment was replaced by a stop codon. The construct was verified by restriction enzyme analysis and sequencing. It was then inserted into a eukaryotic expression vector pRC/CMV (Invitrogen) at the HindIII and XbaI sites. The construct also possesses a cleavable signal sequence (SP/α7AChR) known to target efficiently proteins to the plasma membrane. The cells transfected with the plasmid were incubated at 37 °C in a humidified atmosphere of 5% CO_2 in DMEM (Dulbecco's Modified Eagle Medium, Gibco), containing 10% (v/v) foetal calf serum, 50 IU/ml penicillin, 50 μg/ml streptomycin, and 400 μg/ml geneticin (G418, Gibco BRL).

2.3. Membrane preparation

The confluent cells were washed twice with ice-cold PBS, scraped off the culture dish into ice-cold PBS, and collected by centrifugation at 1000 g for 5 min. The pelleted cells were resuspended in TE (50 mM Tris–HCl, 1 mM EDTA, pH 7.4) with protease inhibitor (Complete Mini, Roche) at an optical density of 0.7 at λ=650 nm. The cells were equilibrated at 4 °C for 10 min at a pressure of 30 atm in a Kontes pressure homogeniser (Avantec) and then disrupted by nitrogen cavitation. The homogenate was centrifuged at 1500 g for 10 min to remove intact cells and nuclei. The supernatant was then centrifuged at 110 000 ×g for 40 min (Beckman rotor type 50.2 Ti). The pellet resulting from the high-speed centrifugation (total membrane fraction: M) was resuspended in TE supplemented with a protease inhibitor cocktail to adjust the protein concentration to about 10 mg/ml.

2.4. Modification of membrane cholesterol content

We performed two experimental procedures to deplete or load cholesterol: to deplete cholesterol from HEK membranes, a volume of the total membrane fraction (M) at a final protein concentration of 0.75 mg/ml in TE containing protease inhibitors was exposed to a concentration of 10 mM (D1) or 20 mM (D2) of MβCD for 1 h at 20 °C and chilled on ice. The MβCD-treated membrane suspensions were then centrifuged in a Beckman centrifuge using a 60Ti rotor at 110 000 g to remove MβCD. The pellets were resuspended in TE buffer resulting in D1 and D2 membranes. To load cholesterol in D2 or in M membranes, the membrane fractions (0.5 mg/ml) were incubated for 30 min at 20 °C under agitation with an equal volume of cholesterol–MβCD complexes and washed as described above to obtain D2+ or M+, respectively. In order to prepare cholesterol–MβCD complexes, a solution of 40 mM MβCD was first prepared in TE. Then, 10 ml of this MβCD solution was warmed at 70 °C and 50 μl of a cholesterol solution (8.6 mg in 100 μl of DMF) was added, resulting in a 1/9 molar ratio of cholesterol/MβCD. The modified membranes were then characterised for protein, phospholipid and cholesterol content, and for binding experiments.

2.5. Binding experiments

Saturation experiments were performed using 5–20 μg of protein of M, M+, D1, D2, and D2+ membranes, in 0.5 ml of 50 mM Tris–HCl, pH 7.4 using [^{3}H]DPN, a non-selective opioid antagonist, or [^{3}H]Del2, a DOR selective agonist. Non-specific binding was determined in the presence of 1 μM unlabelled ligand DPN or Del2. Binding assay experiments were carried out with 100 μM Gpp(NH)p. Following a 1 h incubation period at 25 °C, free ligand was removed by filtration using Whatman GF/B filters. Filters were subsequently washed three times with 10 mM ice-cold Tris–HCl buffer. Radioactivity was measured after adding scintillation fluid and by counting in a Packard Tri-carb 2100 TR. Data were analysed with GraphPad Prism software using a one site binding equation. For competition experiments, [^{3}H]DPN was added at a final concentration of 4 nM with the indicated concentration of unlabelled competitor DPDPE. The results were analysed using one- or two-site binding for the competitor with GraphPad Prism software. The data were best fitted to a two-site competitive binding model, giving the proportion of each population, IC50 values and the resulting DPDPE dissociation constants [23].

2.6. [^{35}S]-GTPγS binding experiments

Membrane preparations (20 μg protein) were incubated in assay buffer (20 mM HEPES, pH 7.4, 100 mM NaCl, 10 μg/ml saponin, 3 mM $MgCl_2$, 0.1% BSA and 1 μM GDP), containing 0.1 nM [^{35}S]-GTPγS, in the presence or absence (basal [^{35}S]-GTPγS binding) of increasing concentrations of DPDPE. Following a 1 h incubation period at 30 °C, free ligand was removed by filtration using Whatman GF/B filters. Filters were subsequently washed three times with cold buffer. Radioactivity was measured after adding scintillation fluid and by counting in a Packard Tri-carb 2100 TR. Agonist efficacy (E_{max}) calculated as the maximal difference between [^{35}S]-GTPγS binding in the presence and absence of DPDPE, and expressed as a percentage of basal and agonist potency (EC50) values were obtained from curve fitting of dose–response curves, using GraphPad Prism software.

2.7. Membrane detergent solubilisation

Solubilisation was assayed using the turbidity of the resulting TX-100-treated membranes (TM). Turbidity of the suspension was measured as absorbance at 500 nm in a Lambda UV spectrophotometer (Perkin-Elmer); the turbidity was also measured as a function of the detergent added, because the gradual solubilisation of lipids result in the disruption of membrane vesicles with subsequent formation of mixed micelles greatly reducing turbidity. Thus, an aliquot of 2 ml of M (0.5, 1, and 3 mg/ml proteins, respectively) was incubated at 4 °C under gentle agitation for 30 min with various concentrations of TX-100 (0.1 to 1%, w/w). We verified that the degree to which membranes were insoluble in detergent remained unaffected even if the treatment was carried out for longer time periods (over-night). This suggests that solubilisation reaches an equilibrium state after 10 min. In subsequent experiments, the M protein concentration was chosen to be 3 mg/ml and then concentrations of TX-100 between 0.1% and 1% were tested.

2.8. Isolation of detergent-resistant membranes (DRMs)

After the solubilisation process, DRMs were isolated by two procedures. In Procedure 1, TM was centrifuged at 100 000 g (TL100 Beckman rotor type TLA100.3)

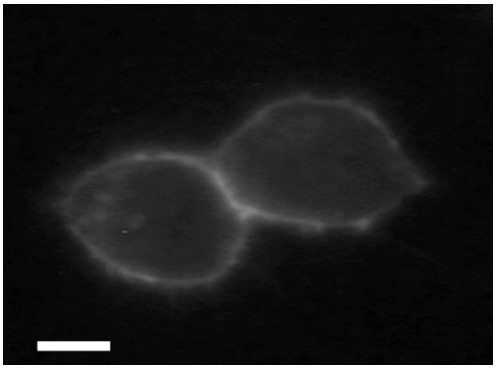

Fig. 1. Fluorescence of eGFP-hDOR (DOR*) in living HEK 293T cells. Wide-field microscope fluorescence image of plasma membranes of HEK 293T cells observed at room temperature, scale bar: 10 µm.

for 20 min to separate the insoluble membranes sedimented in the pellet (P) and the detergent-soluble material in the supernatant (S). S and P (in an equal volume of TE buffer) were either characterised by their protein and lipid content, or deposited on a density gradient. In Procedure 2, TM was deposited on a density gradient. For the density gradient, P, S or TM membranes were mixed with an equal volume of 70% (w/v) sucrose solution. The resulting 40% sucrose fraction was overlaid successively with 4 ml of 30% sucrose and 3 ml of 5% sucrose. The gradient was centrifuged for 18 h at 200 000 g in a Beckman rotor type SW 41 and 1 ml of each fraction (from F_1 to F_{12}) was collected from the top. We determined the turbidity at 500 nm and the sucrose percentage for each fraction. In the samples tested, we observed a light scattering band in the low-density region (F_{3-5}), termed LDF (LDF_P, LDF_S or LDF_{TM}, respectively), and a pellet, termed SP (SP_P, SP_S or SP_{TM} respectively). Each fraction or pooled fractions (LDF, F_{6-11}, SP resuspended with 1 ml TE) were then analysed for quantity of proteins, lipids and presence of DOR*.

2.9. Alkaline phosphatase and protein determination

Alkaline phosphatase activity was determined using *p*-nitrophenylphosphate as a substrate. A 100 µl aliquot of each gradient fraction was added to 1 ml of 200 mM Tris buffer, pH 10.2 containing 4 mM $MgCl_2$, 275 mM mannitol, and 16 mM *p*-nitrophenylphosphate. After a one-hour incubation at 37 °C, the absorbance was measured at 405 nm (Zeiss PMQII spectrophotometer). The measured absorbance in LDF_{TM} and SP_{TM} were converted per unit mass of the fraction of protein to give specific activity. Protein content was measured according to Lowry et al. [24] with bovine serum albumin as standard.

2.10. Lipid analysis

Lipids from M, S or P membranes and density gradient fractions were extracted according to the Bligh and Dyer procedure [25]. The cholesterol content was measured using a colorimetric method (Roche Molecular Materials) or according to the Zak protocol [26]. Phospholipids (PL) and sphingomyelin were titrated according to the Rouser procedure [27]. The lipid composition of the lipid extracts was characterised: the various lipid extracts were spotted on TLC plates and submitted to migration with chloroform/methanol/water (65:25:4, by vol.). The plate was dried and the spots were revealed by spraying with sulphuric acid and heating at 250 °C for 15 min. The spots were quantified using a range of lipid standards and were analysed by ImageJ Software.

2.11. DOR* quantification as a result of fluorescence measurements

DOR* quantities in the membrane fractions (M, P, LDF, SP) were estimated by steady-state fluorescence measurements, carried out with a 500 SLM-Aminco spectrofluorometer. The excitation wavelength was set to 475 nm and fluorescence emission was measured over a wavelength range of 490–550 nm. Measurements were made with solutions of membrane fractions resuspended in TE buffer, and the protein concentration adjusted between 0.1 and 0.6 mg/ml; this ensures that the fluorescence signals were in a measurement range of a defined instrument setting. We evaluated the specific fluorescence intensity of eGFP between 500 nm and 535 nm and we calculated the contribution of light scattering and inner filter effects on the spectra according to the following conceptual set up [28]. According to the Rayleigh–Gans–Debye theory, light scattering for liposome suspensions can be described by Eq. (1), in which the parameters A(1) and A(0) are to be adjusted:

$$A(\lambda) = A(1)/\lambda^4 + A(0). \quad (1)$$

In our study, we deduced an empirical equation (Eq. (2)) from Eq. (1). Eq. (2) fits the light scattering of our membrane suspensions where λ indexes the wavelength in the range between 490–500 nm and 535–550 nm. A(0), A(1) and A(2) are parameters to be adjusted:

$$A(\lambda) = A(1)/(\lambda - 490)^{A(2)} + A(0). \quad (2)$$

Calculations were performed using a non-linear regression program, GraphPad Prism. The confidence intervals for the estimated parameters corresponded to an error risk of 5%. Accordingly, removing the baseline profile from spectra between 490 nm and

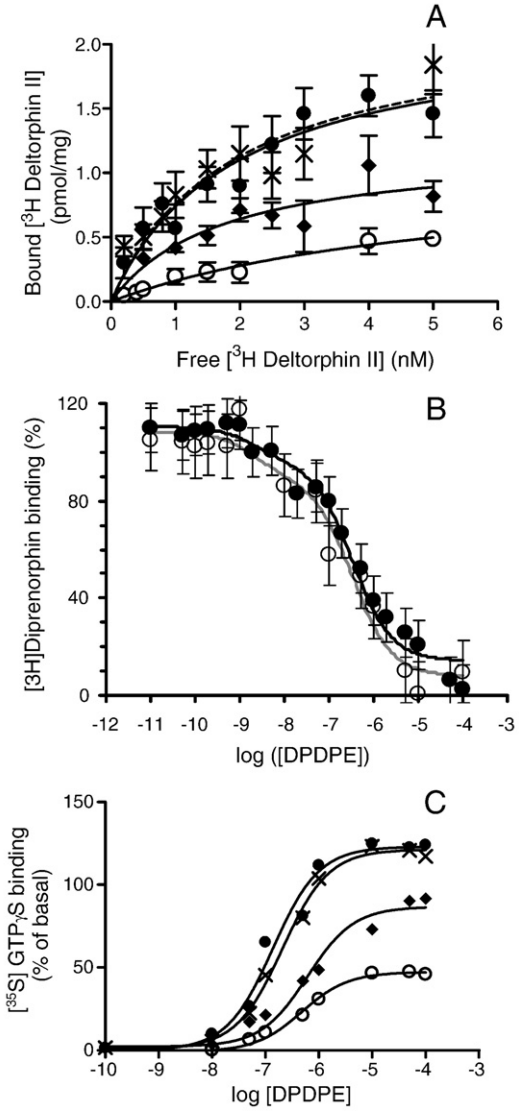

Fig. 2. Effect of cholesterol content on DOR* activity in HEK 293T membranes. M membranes are depleted in cholesterol using 10 mM or 20 mM MβCD, as described in Materials and methods. The corresponding values for measured Chol/PL are 37% in M (●), 13% in D1 (♦) or 8% in D2 (○). The D2 membranes are then re-complemented with cholesterol-loaded MβCD, leading to a Chol/PL of 92% in D2+ membranes (×). A: Specific Del2 binding is measured, as described in the Materials and methods section. Data were analysed with a non-linear regression and were best fit by a monophasic hyperbola. The figure represents one of the three experiments performed in duplicate with similar results. Similar data were obtained for other membrane preparations. The pharmacological parameters obtained are given in Table 1. B: Competition binding of DPDPE. Competition displacement experiments were performed on M and D2 membranes. [^{3}H] DPN was used at a final concentration of 4 nM. The best fit was obtained by a two-site competitive binding model, yielding dissociation constants of 1.85±0.3 nM and 210 ±22 nM; the fractions of M membranes (grey bars) and D2 (black bars) in high affinity were 28±4% and 33±4%, respectively. C: Dose–response curves for DPDPE-stimulated [35S]GTPγS incorporation in the M and D2 membranes. Agonist efficacy (E_{max}) was calculated as the maximal difference between the presence and absence of DPDPE and is expressed as a percentage of the basal value. Agonist potency (EC50) values were obtained from curve fitting of dose–response curves. The values are means±S.E.M. of two experiments performed in duplicate.

550 nm enabled us to obtain the fluorescence intensity of eGFP (ΔF), measured at 512 nm (Fig. 3B).

We carried out the following approach to correlate the DOR* number in M membranes, estimated by means of measurements of the receptor quantity able to bind in high affinity the antagonist DPN, with the quantity of DOR* estimated by its fluorescence response. We quantitatively measured the fluorescence response of DOR* fractions by comparing it with a reference standard, the NBD-PA, which fluoresces at a similar wavelength range to that of the fluorophore eGFP. We then used the approach described by Lakowicz [29]. It was defined by the following equation:

$$C_{eGFP} = (\varepsilon_{ref}/\varepsilon_{eGFP}) \cdot (\phi_{ref}/\phi_{eGFP}) \cdot (If_{eGFP}/If_{ref}) \cdot (C_{ref}) \cdot (n^2_{eGFP}/n^2_{ref}), \quad (3)$$

ϕ is the quantum yield, If is the fluorescence intensity and ε is the molar absorption coefficient of the reference (NBD-PA)[30] or DOR* (eGFP) suspensions at similar apparatus settings, n is the refractive index of the environment surrounding eGFP (water) or the reference (chloroform). The following values were used: ϕ_{ref}=0.05, ε_{ref}= 10 000 $M^{-1}\cdot cm^{-1}$ [30], ϕ_{eGFP}=0.6, ε_{eGFP}=55 000 $M^{-1}\cdot cm^{-1}$ [31]. n^2_{eGFP} and n^2_{ref} were the refractive indexes of water and chloroform [32].

3. Results

We prepared a recombinant human embryonic kidney cell line, which expresses a stable form of hDOR fused to eGFP in C_{term} and can be detected by fluorescence. We verified by optical microscopy that the recombinant hDOR (DOR*) exhibited mainly plasma membrane localisation (Fig. 1). The aim of our study was to investigate the role of rafts in DOR* activity using only membrane preparations preventing any events induced by cellular processes (i) by analysing the influence of membrane cholesterol content on DOR* ligand binding capacities and (ii) by measuring DOR* partitioning in separated membrane fractions.

3.1. DOR* functionality and its membrane quantifications

We tested the functionality of DOR* (Fig. 2A, B, C) by examining its ability to bind its ligands in the membrane preparations: A receptor amount of 6.5 pmol/mg and a K_d of 1.3 nM were determined by the DPN binding experiments (Table 1). Within the agonist, Del2, concentration range explored (Fig. 2A, Table 1), a single population corresponding to a pool of 2.1 pmol/mg of the receptor was observed to be in the high affinity state (K_d=1.9 nM). Competition curves for binding between [^{3}H]DPN and unlabelled DPDPE, another specific DOR full agonist, and the data obtained by modelling the curves with two populations are given in Fig. 2B. Also, the proportion of sites in the high affinity state (28%) is consistent with the percentage of the total receptor pool labelled by [^{3}H]Del2 (Table 1). Our findings indicated that the high binding affinities of these three ligands are consistent with those reported previously for the wild-type receptor [33,34].

Steady-state fluorescence measurements allowed the quantification of the receptor concentrations in the basal membranes or various membrane fractions obtained by solubilisation preparations. To finalize this protocol, for calibrating the eGFP of hDOR fluorescence in membranes, we used the emission spectra from a range of increasing protein concentrations of M (0.1 to 0.6 mg/ml) (Fig. 3A). For each suspension, fluorescence intensity, ΔF, was plotted as a function of the amount of proteins (Fig. 3C). This demonstrates a proportional relation between ΔF and the protein concentration (4.15 a.u./mg of M). We estimated the concentration of the eGFP fluorophore using NBD-PA as the standard fluorescent reference [30]: we evaluated a value of 8±3 pmol/mg. It is in a same range of that determined by pharmacological binding of DPN. Furthermore, assuming a value of 6.5 pmol/mg of membrane proteins obtained in the antagonist binding measurements for active DOR* receptor (Table 1), the ΔF values can be related to a number of initial receptors (Fig. 3C). We calculated a slope of 0.64 a.u./pmol of receptor. This result allowed us to quantify DOR* in the various membrane fractions studied.

3.2. Modulation of DOR* binding activity by the membrane cholesterol content

We examined the influence of cholesterol content on DOR* activity by measuring Diprenorphine and Del2 binding or DPN displacement by DPDPE, in membranes in which the cholesterol content was modified. Above all, we verified using eGFP fluorescence quantification that the membrane receptor content was unchanged after MβCD treatment (Fig. 3D). An enrichment in cholesterol (Table 1: M+ with Chol/PL=64% mol/mol) did not modify the binding parameters (B_{max} and K_d) of both ligands. By contrast, by increasing the MβCD concentration, the cholesterol content progressively decreased (Fig. 2A, Table 1). Table 1 gives the dissociation constants (K_d) and the B_{max} values obtained with the two ligands in MβCD-treated membranes (D1 and D2) and in non-treated membranes (M). Comparison of B_{max} values, obtained within the range of concentrations tested with Del2 (1 pmol/mg) and DPN (2.6 pmol/mg) in D2 membranes, suggests that 38% of the receptors are in a high affinity state. When competition displacement experiments were performed on D2 membranes, with [^{3}H]DPN as ligand and DPDPE as competitor (Fig. 2B), the data obtained with D2 were consistent with two populations with similar K_i values and proportionally similar (33%) to that obtained with M membranes. These data, consistent with the results obtained by [^{3}H]Del2 binding, suggest that the cholesterol content modulates the low and the high affinity state. However, even with a very low Chol/PL ratio (8%), 40% and 47% of the total receptor pool remains able to bind DPN and Del2 respectively, with very similar binding affinities. Moreover, the depleted membranes were re-complemented in cholesterol (D2+) to check whether the effects of MβCD treatment on receptor binding could be reversed. In D2+, the receptor binding factors and responses were fully restored.

We also analysed the influence of G-protein coupling on Del2 binding in M and D2 by adding GppNHp in binding assays (Table 1). The data shows that the pool of receptors recognised by Del2, within concentration range explored, corresponds to 1.6 pmol/mg and 0.3 pmol/mg, i.e. 25% and 5% of the total receptor pool (6.5 pmol/mg) in M and D2, respectively. These data show that the fraction of receptors in high affinity state (labelled by [^{3}H]Del2) is, as expected

Table 1
Binding parameters of DOR* expressed in M membranes in which cholesterol content was modified using MβCD

Samples	Chol/PL (%)	Diprenorphin (DPN)			Deltorphin II (Del2)							
					− GppNHp				+GppNHp			
		B_{max} (pmol/mg)	B_{max} (% of M)	K_d (nM)	B_{max} (pmol/mg)	B_{max}[a] (%)	B_{max}[b] (%)	K_d (nM)	B_{max} (pmol/mg)	B_{max}[a] (%)	B_{max}[b] (%)	K_d (nM)
M	37±3	6.5±0.5	100	1.3±0.4	2.1±0.3	100	32±8	1.9±0.7	1.6±0.2	100	25±5	5.5±1.8
D1	13±2	3.0±0.3	46±8	1.2±0.3	1.3±0.2	62±15	20±4	2.0±0.4	n.d.	n.d.	n.d.	n.d.
D2	8±0.5	2.6±0.4	40±8	1.6±0.6	1.0±0.1	47±11	15±2	5.5±1.8	0.3±0.1	18±8	5±3	2.0±1.1
D2+	92±16	6.8±0.6	104±18	2.2±0.5	2.1±0.4	100±13	30±10	1.8±0.8	n.d.	n.d.	n.d.	n.d.
M+	64±10	6.0±0.6	92±15	2.0±0.6	1.9±0.3	90±15	29±10	1.0±0.6	n.d.	n.d.	n.d.	n.d.

Data correspond to mean values±S.E.M. of three doubled independent experiments.
n.d.: not determined.
[a] Percentage of B_{max} value evaluated from the sample M as reference.
[b] Percentage of B_{max} value evaluated from the total receptor pool calculated by [^{3}H]DPN in M samples (6.5 pmol/mg).

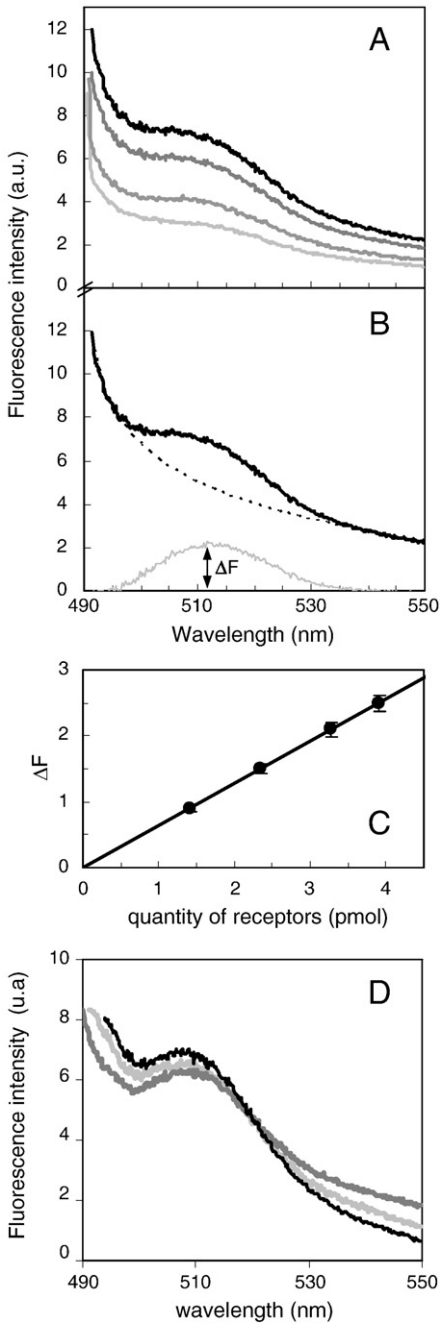

Fig. 3. Quantification of DOR* in M membranes. (A) Fluorescence spectra of eGFP of M membranes at 0.25 mg/ml, 0.35 mg/ml, 0.5 mg/ml, and 0.6 mg/ml (from top to bottom). (B) Fluorescence spectrum of eGFP of M membranes at 0.6 mg/ml (black line) and baseline fit obtained by non-linear regression using Eq. (2) (dotted line). Corrected eGFP fluorescence spectra (grey line) were obtained by removing the fit to the original spectra. The resulting maximum fluorescence intensity (ΔF) was measured at 512 nm. (C) Evolution of ΔF as a function of the protein concentration. A proportional relation of ΔF with protein concentration is obtained (0.45 a.u./mg of M membranes). Assuming a B_{max} of 6.5 pmol/mg of M membranes for Diprenorphine, ΔF can be expressed as a function of DOR* binding capacity with a slope of 0.64 a.u./pmol. (D) Fluorescence spectra of native M membrane (grey sinks), after cholesterol depletion (light grey), or after cholesterol re-complementation (black).

[34], lower in the presence of GppNHp but also that 78% of depletion of cholesterol in the membranes (Table 1: M→D2) caused 82% of inhibition of the high affinity state receptor pool.

Moreover, incorporation of the non-hydrolysable GTP-analog [^{35}S]-GTPγS in M, D1 and D2 membranes was used to monitor the influence of membrane cholesterol depletion on agonist-induced stimulation. The ability of DPDPE to activate G-protein is decreased in D1 (30% of the E_{max} value of M) and D2 (50% of the E_{max} value of M) without significantly affecting EC_{50} values (Fig. 2C). Also, the lower E_{max} values in D1 and D2 are in accordance with fewer numbers of receptors in a high affinity state.

3.3. Solubilisation, isolation and characterisation of detergent-resistant membranes (DRMs)

3.3.1. Membrane detergent solubilisation

We investigated whether DOR* was partially localised in cholesterol-rich microdomains; thus, we analysed its partitioning between DRMs and solubilised membranes (N-DRMs) after cold TX-100 treatments. Assuming that the extent of membrane solubilisation depends essentially on the detergent to lipid ratio, the solubilisation process was analysed by measuring changes in turbidity as a function of the detergent added (Fig. 4A). As expected, the ability of TX-100 to solubilise was enhanced with increasing detergent concentrations or by lowering membrane concentrations. However, in contrast to SDS solubilisation of membranes or cold TX-100 solubilisation of liposomes [35], the suspensions never completely cleared, even at the highest concentration of detergent.

3.3.2. Isolation of membrane fractions and characterisation

We compared DRMs obtained from two procedures using various TX-100 quantities. In Procedure 1, treated membranes (TM) were centrifuged resulting in a pellet (P) and supernatant (S), corresponding to unsolubilised membrane and soluble material, respectively. Each fraction was then subjected to a discontinuous sucrose density

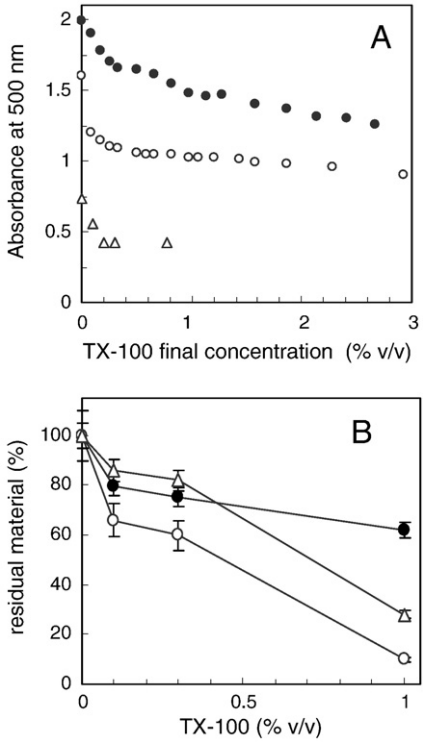

Fig. 4. Solubilisation and characterisation of protein, PL and cholesterol contents of membranes with increasing TX-100 concentrations. A: M membranes were treated with aliquots of a concentrated solution of TX-100 at 4 °C with constant stirring for 10 min. The turbidity of TM was measured at an absorbance of 500 nm. Solubilisations were performed with 3 mg/ml (●), 1 mg/ml (○) and 0.5 mg/ml (△) of M membranes. B: M membranes (3 mg/ml) were treated with various concentrations of TX-100 for 30 min at 4 °C. The resulting TM membranes were sedimented by ultracentrifugation at 100 000 ×g for 20 min at 4 °C (Procedure 1). Each pellet (P) was resuspended in an equal volume of TE buffer and the phospholipid (○), protein (●) and cholesterol (△) contents were measured. The corresponding PL/protein ratios expressed in nmol of PL per mg of proteins are given in Table 2.

Table 2
Measured PL/protein, Chol/PL and SM/PL ratios in samples obtained by fractionation of TM

TX-100 (%)	PL/protein (nmol/mg)			Chol/PL (% mol/mol)				SM/PL (% mol/mol)		
Samples:	0	0.1	1	0	0.1	0.3	1	0	0.1	0.5
M	350±60			37±3				2.4±0.5		
P		188±32	42±7		58±5	71±6	109±11		1.3±0.3	13±3.0
S		368±62	826±140		19±2	23±2	27±3		0	0
LDF_{TM}		4670±800	1710±290		65±6	73±7	66±6		5.8±0.6	11.5±2.0
$(F_{6-11})_{TM}$		441±70	423±72		35±3	46±4	46±5		2.4±0.5	1.4±0.3
SP_{TM}		158±26	34±6		41±4	55±5	50±5		5.1±1.0	8.4±1.6

Data correspond to mean values±S.E.M. of three independent experiments.

gradient, to check for heterogeneity in composition; in Procedure 2, TM membranes were subjected directly to a discontinuous sucrose density gradient. The first step of Procedure 1 is classically used to estimate solubilisation of HEK membranes by measuring the amount of phospholipids and protein present in P and S. The data indicated a progressive loss of membrane phospholipids in P (Fig. 4B). A large proportion of membrane phospholipids were solubilised (90% PL) at the highest concentration of detergent used (1%). However, the results for membrane proteins show efficient solubilisation of protein (20%) at low concentrations of TX-100 (0.1%), beyond which greater concentrations of detergent cause only a weak increase in the extent of solubilisation: 70% of the protein content remained in the pellet. The resulting PL/protein ratio (Table 2) in S increases with increasing TX-100 concentration (368 and 826 nmol/mg for 0.1% and 1%, respectively). By contrast, the ratio decreases in P: with 1% TX-100 treatment, the PL/protein ratio was significantly lower (Table 2: 42 nmol/mg) than the initial value (350 nmol/mg), indicating that the samples obtained in pellets under these conditions are very poor in lipids.

We then submitted P to a sucrose gradient, and observed a light scattering band in the low-density region (LDF_P) and a sucrose-pellet (SP_P), under all solubilisation conditions. LDF_P, $(F_{6-11})_P$ and SP_P were collected and individually assayed for protein and lipid content. The data obtained with 0.1% TX-100 are shown in Fig. 5A. We noted that 65% of TM protein content was collected in SP_P, but only 2.5% was collected in LDF_P. A similar amount of lipid was recovered in LDF_P, $(F_{6-11})_P$ and SP_P. $(F_{6-11})_P$ was subjected to a second ultracentrifugation step to explain the presence of insoluble material in these fractions, usually attributed to soluble material. In this case, lipids and proteins are found exclusively in the pellet (data not shown). Therefore, $(F_{6-11})_P$ contains insoluble membranes, which probably differ from LDF_P and SP_P in their intrinsic density.

We subjected the S sample to the sucrose gradient: no pellet (SP_S) was observed (Fig. 5A). Only a small band was sometimes observed in LDF_S (PL<5%) (Fig. 5B, C). As expected, proteins and lipids were mostly recovered in $(F_{6-11})_S$.

We compared Procedure 1 to one more classically used to isolate DRMs: Procedure 2. In this case, a light scattering band in LDF_{TM} and SP_{TM} was observed with various TX-100 concentrations. Proteins were mainly present in SP_{TM} (72%), whereas only 4% was present in LDF_{TM} (Fig. 5A). By increasing TX-100 concentrations, we observe a progressive loss of protein and lipid in the SP_{TM}, whereas the lipid and protein content increase in $(F_{6-11})_{TM}$ (data not shown). In LDF_{TM}, a near constant protein amount was observed; however, the PL/protein ratio (Table 2) decreased with increasing TX-100 concentrations (from to 4670 to 1710 nmol/mg with 0.1% and 1% TX-100, respectively), indicating a progressive loss of lipids in LDF_{TM}. As expected by fraction localisation across the gradient, LDF_{TM} has a higher PL/protein ratio than SP_{TM} (≈158–34 nmol/mg) and even that of M membranes (350 nmol/mg). M membranes were regrouped in the sucrose-pellet, if subjected to this sucrose gradient.

We analysed the P, S and the TM gradient fractions for the presence of raft protein and raft lipid markers. This analysis was carried out to further characterise the specificity of detergent resistance in relation to the significance of rafts. The presence of raft proteins markers, such as the acylated protein Alkaline phosphatase (PLAP) known to be selectively enriched in rafts [36], was detected in LDF_{TM} and in SP_{TM} (Fig. 6). The resulting specific activities of samples solubilised with 0.1% TX-100 were 1.7 a.u./mg and 0.3 a.u./mg for LDF_{TM} and SP_{TM}, respectively, suggesting that LDF_{TM} is enriched in PLAP.

The distribution of cholesterol (Fig. 5) and the corresponding Chol/PL ratios are given in Table 2. At 0.1% of TX-100, cholesterol is almost exclusively found in P. Also, Chol/PL values in P (58%), LDF_{TM} (65%), and SP_{TM} (41%) were higher than those measured in S (19%) or in M membranes (37%). Chol/PL values were greater with increasing TX-100

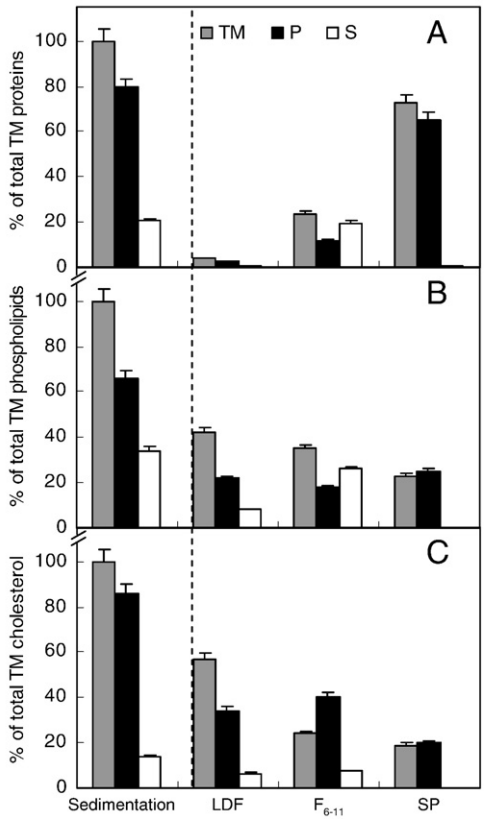

Fig. 5. Lipid and protein contents in samples obtained by fractionation of TM using 0.1% TX-100. TM (grey bars) was obtained according to M membrane treatments (3 mg/ml) with 0.1% TX-100. After the solubilisation procedure, TM was separated in two samples. In the left part of the panel according to Procedure 1: the first sample was centrifuged at 100 000 ×g for 20 min at 4 °C giving rise to a pellet P (black bars) and a supernatant S (white bars), in which protein (A), phospholipid (B) and cholesterol (C) contents were measured. In the right part of the panel, P and S were then subjected to a density gradient leading to LDF_P, $(F_{6-11})_P$, SP_P and to LDF_S, $(F_{6-11})_S$, SP_S respectively. According to Procedure 2: the second sample was directly subjected to the same density gradient, resulting in LDF_{TM}, $(F_{6-11})_{TM}$ and SP_{TM}, depicted by the corresponding grey bars which characterise their lipid and protein contents. Data are means±S.E.M. of two experiments performed in duplicate.

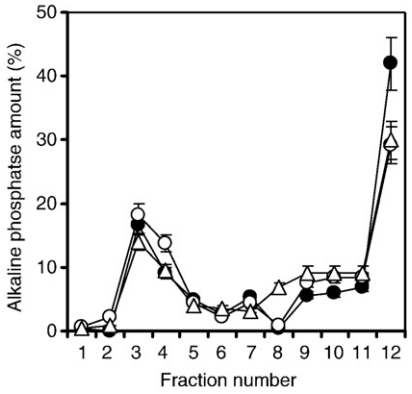

Fig. 6. Distribution of PLAP in the sucrose gradient fractions of TM membranes. TM membranes were obtained by treatment of M membranes with 0.1% (●), 0.3% (○) and 0.5% (Δ) of TX-100. TM was subjected to a density gradient (Procedure 2). Each gradient fraction was assayed for protein content and for alkaline phosphatase activity. The resulting specific activities were 1.7 ± 0.3 a.u./mg and 0.3 ± 0.1 a.u./mg in LDF_{TM} and SP_{TM}, respectively.

concentrations, indicating that the membranes were not homogeneously solubilised by cold TX-100. In all cases, LDF_{TM} was more enriched with cholesterol than SP_{TM}. We carried out an extensive analysis by determining the composition of lipid species in several fractions obtained under various extraction conditions (0.1% TX-100: Fig. 7A and 0.5%: Fig. 7B). First, P, LDF_{TM} and SP_{TM} displayed similar compositions. We observed the following patterns of solubility: PS, PG and SM (sphingomyelin) appeared to be weakly soluble (only observed

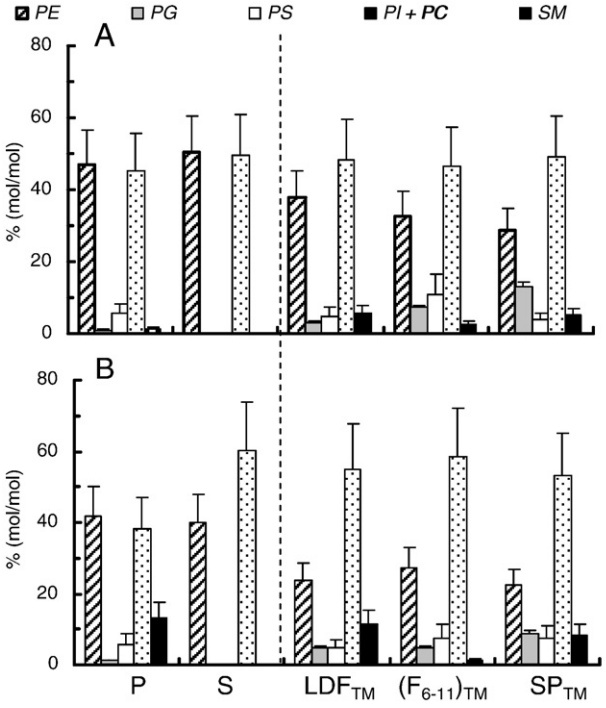

Fig. 7. Characterisation of the lipid composition in samples obtained by fractionation of TM. M membrane solubilisations were performed with 0.1% (A) or 0.5% (B) of TX-100. S and P membranes were obtained by sedimentation of TM, as described in the Materials and methods section (First step of procedure 1). TM was solubilised with 0.1% (A) or 0.5% (B) of TX-100 (Procedure 2). TM was then subjected to the density gradient, and LDF_{TM}, $(F_{6-11})_{TM}$ and SP_{TM} were subsequently collected after fractionation. The lipid compositions were obtained by a TLC analysis of each sample. The quantification of lipid species was performed by measuring the intensity of each spot compared with the corresponding lipid standard. The data are expressed as a percentage of the total amount of lipids in a given fraction. Data are means ± S.E.M. of three experiments. PE (phosphatidylethanolamine), PG (phosphatidylglycerol), PS (phosphatidylserine), PI (phosphatidylinositol), PC (phosphatidylcholine), and SM (sphingomyelin).

in P) in cold TX-100. PI-PC was in turn more soluble than PE (an increase in the TX-100 concentration results in greater amount of PI-PC in S), consistent with previous studies [37,38] (Fig. 7A, B). Furthermore, a marked difference between $(LDF/SP)_{TM}$ and soluble material (S) was a higher SM/PL value, which increases with increasing TX-100 concentrations (Table 2). By contrast, the data obtained with $(F_{6-11})_{TM}$ in comparison with S confirmed reported contamination by insoluble material in $(F_{6-11})_{TM}$, and in this way, the difficulty encountered in analysing this sample.

3.4. hDOR partitioning

We investigated DOR* partitioning in membranes using various TX-100 concentrations. Assuming that eGFP has a similar environment in M as in DRMs (P, LDF, SP), DOR* can be quantified by eGFP analysis (Fig. 3). However, soluble fractions of membranes cannot be quantified by the same procedure. Thus, the balance in the distribution of DOR* was obtained by comparing Δ*F* values of deposited membranes and its Δ*F* values that correspond to the insoluble membrane fractions

We compared the fluorescence intensities of samples S and P obtained by sedimentation of membranes treated with various concentrations of detergent. The data showed an increase of the fluorescence intensity in S with increasing TX-100 concentrations, correlated with a decrease of the fluorescence in P, indicating progressive DOR* solubilisation. However, no clear difference was observed between the fluorescence of fractions with 0.5% TX-100 and samples with concentrations of TX-100 above 0.5%; this correlates with the protein solubilisation process (Fig. 2) and suggests that DOR* solubilisation is maximal with about 0.5% TX-100 and 3 mg/ml of membranes.

We estimated the amount of receptors in P obtained from the two series of experiments, in which M was treated with 0.1% or 0.3% TX-100 (Fig. 8). Almost 30% of the initial DOR* amount was retrieved in P if 0.1% TX-100 is used. It decreased to 23% with 0.3% or 1% of TX-100, suggesting that total solubilisation of DOR* was never observed. P was then subjected to a density gradient. The percentages of initial DOR* in LDF_P and in SP_P using the lowest concentration of TX-100 are 5% and 24%, respectively, and not detectable fluorescence was observed in $(F_{6-11})_P$. At a concentration of 0.3% TX-100, only 3% of receptors were measured in LDF_P and increasing detergent concentration causes the loss of the receptor from LDF_P; however, 14% of receptors were still present in the SP_P fraction (Fig. 8). These last results are in agreement with data obtained with Procedure 2: DOR* was observed in $(F_{6-11})_{TM}$, in SP_{TM} and was only detectable in LDF_{TM} if a low TX-100 concentration (0.1%) was used (data not shown).

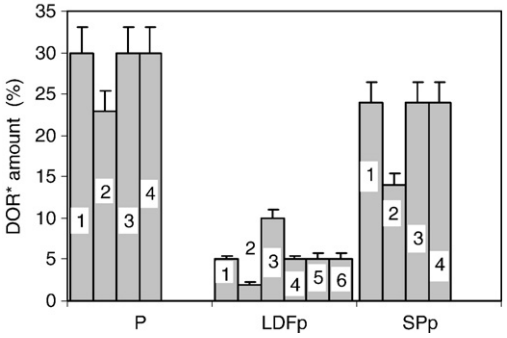

Fig. 8. Percentage of total DOR* in DRMs isolated, according to the Procedure 1. eGFP fluorescence was estimated in P, LDF_P and SP_P and correlated with a quantity of initial DOR*, as described in Fig. 3. The bars corresponded to: 1) M membranes solubilised with 0.1% of TX-100, 2) M membranes were solubilised with 0.3% of TX-100, 3) M membranes solubilised with 0.1% of TX-100 + DEL II, 4) M membranes were solubilised with 0.1% of TX-100 + DPN, 5) M membranes solubilised with 0.1% of TX-100 + DEL II + GppNHp, and 6) M membranes solubilised with 0.1% of TX-100 + GppNHp. The data represented the mean of two independent experiments.

We also investigated the effect of the DOR* micro-localisation in regulating its function. We then studied the effect of ligand addition and of GppNHp addition on DOR* partitioning; this was carried out by resuspending M membranes, before and during cold extraction, in buffer containing an excess of either Del2 or DPN, in the absence or presence of GppNHp. We measured the amount of receptors in LDF_P and SP_P in these cases (Fig. 8). Del2 treatment led to a two-fold increase in the amount of DOR* in LDF_P (5% to 10%), whereas no change was detected in SP_P. This last result was confirmed by checking the effect of adding Del2 on the amount of DOR* in P, assuming that SP_P contains more DOR* than LDF_P: no modification of the P content was observed upon the addition of ligand. In addition, Del2 systematically resulted in an increased amount of DOR* in LDF_{TM}, as analysed using Procedure 2 (data not shown). However the addition of GppNHp prevented any redistribution of DOR* (Fig. 8), suggesting that G-protein coupling is required in LDF_P or LDF_{TM} enrichment. Also, no difference in fluorescence was observed in P, in LDF_P or in SP_P after the addition of DPN.

4. Discussion

The purpose of our study was to investigate the correlation between DOR* activity and its localisation in cholesterol-enriched microdomains.

4.1. Characteristics of DRMs isolated by various procedures

We investigated the presence of cholesterol-enriched microdomains in HEK membranes using two extraction methods based on their cold TX-100 insolubility (Procedure 1, or Procedure 2). If we compare the protein and lipid content of P with LDF_{TM} and SP_{TM}, we observe that the protein content of LDF_{TM} and SP_{TM} is in fact derived from P. Finally, Procedure 1 appears to be the best approach for analysing soluble (S) and insoluble (LDF_P, SP_P) materials.

Overall, our results show that unsolubilised membranes (P, LDF, SP compared with S) were enriched in cholesterol and sphingomyelin. We observed an increase in these lipid species with the use of increasing TX-100 concentrations. Detergent insolubility was also observed in this study, consistent with previous reports [4]: it may be explained by the existence of microdomains with various physico-chemical properties, allowing specific and distinct intermolecular interactions with the detergent, thus resulting in the differential solubilisation of these microdomains. In the *lo* phase microdomain, the properties of detergent resistance are attributed to close packing of saturated acyl-chains of sphingolipids stabilized by cholesterol. Recent experiments clearly indicate that the use of TX-100 provides the ability to distinguish between the *ld* and *lo* lipid phases by selectively solubilising the *ld* phase, yet *lo* domains may be contaminated with additional lipids from the *ld* phase [14]. In our study, the experiments support the existence of sphingomyelin-rich and cholesterol-rich domains in HEK membranes.

However, by DRM fractionation, insoluble material was isolated in LDF but also in SP, and the percentage of protein in LDF (2–5% of the protein content) appeared to be significantly lower than that in SP (50–70% of the protein content). Similar observations were made with membranes of CHO cells expressing hMOR (Gaibelet et al., submitted manuscript). In another study whose aim was to characterise microdomains of mouse thymocytes using Brij 98 at 37 °C, 2.5% of total protein was detected in low-density detergent-insoluble membranes [39]. We observed that PLAP was also associated with LDF_{TM} and SP_{TM}, with higher levels of enrichment in the LDF_{TM} than in the SP_{TM}. Taken together these data indicated that LDF and SP exhibit classic biochemical raft characteristics.

Few studies have reported unsolubilised material in SP. Cytoskeleton elements were thought to be responsible for the insolubility of these particular membranes [40,41]. However, it must be emphasised that (i) actin cytoskeleton may be prominent in constructing rafts [42]; also, (ii) actin has been shown to be associated with DRMs of low density, if a low detergent concentration is used, and it has been found sedimented in the sucrose-pellet after the detergent concentration was increased. The data also suggested that high density fractions contain both non-raft and raft materials [15]. Furthermore, even if rafts are classically defined as a domain of low density, reported rafts do not appear to be identical in terms of their protein or lipid content, and are dependent on the type and concentration of the detergent used and on the cell type. Also, DRMs of various compositions can be generated from the same starting material using one simple non-ionic detergent and a graded extraction of membrane-associated proteins, in which protein-raft markers are observed by increasing detergent concentrations [15]. Indeed, it is likely that a given protein can associate with rafts with various kinetics or partition coefficients. As a consequence, the solubilisation may be based not only on their differential spatial distribution within raft and non-raft microdomains, but also on their individual chemical properties [13]. Thus, lipid raft isolation that does not involve detergent extraction has been developed to assess the possible introduction of artefacts through detergent use [43]. Interestingly, both procedures result in similar conclusions, yielding membrane fractions of low density, highly enriched in cholesterol, glycosphingolipids and a variety of proteins thought to be protein-raft markers [44].

Finally, the reported variability in DRM composition could be explained by the co-existence of multiple, distinct, co-existing raft domains within the plasma membrane [1]. In our study where LDF exhibited classic biochemical raft characteristics, it is difficult to consider that all proteins in SP (~70%) constitute pre-existing raft proteins. SP appears to be more of an aggregate of proteins containing raft markers and would correspond to membrane domains which were disrupted. These data suggest that detergent extraction does not allow the separation of all the various lipid domains. Many studies have sought to characterise DRMs, but defining the best conditions to specifically extract maximum rafts appears to be difficult [15].

4.2. DOR* partitioning

No significant and reproducible binding activity was observed in the various fractions obtained, using our solubilisation and DRMs fractionation conditions (according to Procedure 1 or 2). Fortunately, eGFP allowed us quantitative steady-state fluorescence measurements of DOR* in the membrane fractions (M, P, LDF and SP). This approach shows its efficiency in the quantification of eGFP-labelled DOR in various membrane samples analysed.

Overall, in the HEK membranes, we found that >70% of the initial pool of DOR* can be extracted by TX-100; however, it is only with the lowest TX-100 concentrations that DOR* appeared to be associated with LDF. The addition of DPN and GppNHp had no effect on the DOR* distribution between DRMs and non-DRMs, but a two-fold increase of DOR* content in LDF_P was induced by Del2, and was prevented by the addition of GppNHp. These data suggest that the form able to shift into LDF is the high affinity state form, stabilized by its interaction with G-protein [45].

In contrast to our results, a recent study using a detergent-free method has shown that about 70% of DOR are present in DRMs of low density. Furthermore, stimulation with full agonist, but not with partial or inverse agonists, shifts 25% of DOR out of the rafts [46]. However, the method used replaces non-ionic detergent with a high pH sodium carbonate buffer, a protocol previously proposed for the isolation of caveolae.

Caveolae are morphologically and biochemically characterised [47–49]. They appear to exist predominantly at the cell surface as independent and defined structures [50]. It would seem that membrane lipid rafts could be precursors of caveolae, but caveolae have other specific precursor proteins, such as caveolin, and cannot be defined as rafts.

Interestingly, our data are consistent with those Alves et al. [20]: they observed a dynamic recruitment of hDOR upon agonist binding from the PC-rich to the SM-rich domain in a planar-supported bilayer composed of a PC/SM mixture. Also, hDOR trafficking with antagonist treatment was 2-fold lower than that with agonist treatment.

4.3. Characteristics of DOR binding activity and modulation of this activity by the membrane cholesterol content*

After MβCD cholesterol depletion, we observed that DPN and Del2 B_{max} values and also the amount of agonist-induced [^{35}S]-GTPγS incorporation decreased gradually with a decrease in the cholesterol content. These experiments support a regulatory role for cholesterol in DOR* activity. It is clear that cholesterol plays an important role in modulating several GPCRs functions. An increase in the amount of cholesterol has an inhibitory effect on rhodopsin function [51]. By contrast, several GPCRs appear to require cholesterol for agonist binding function [52]. Experiments with the hippocampal serotonin-1A receptor demonstrate that the reduction of membrane cholesterol content significantly attenuates not only agonist binding but also its antagonist binding function [53]. This was also the case for DOR* in this study. Furthermore, this effect can be reversed and the decrease in B_{max} is not due to the loss of receptors from the plasma membrane (eGFP fluorescent measurements). Overall, our experiments show that almost 60% of the total receptor, in which 15% is in high affinity state, required cholesterol for binding activity (Table 1). They suggest the existence of at least four pools of DOR* (B^{b}_{max} Table 1): Two pools requiring the presence of cholesterol for a conformation able to bind its ligand (agonist and antagonist): (i) one pool in high affinity state (~15%) and (ii) one pool in low affinity state (~45%). Two others pools which may be stabilized in a cholesterol-poor environment: (i) one pool in high affinity state (~15%) and (ii) one pool in low affinity state (~25%). Moreover, experiments carried out in the presence of GppNHp destabilized the equilibrium between the two forms (high and low affinity state). They showed that, if the membrane contained 8% Chol/PL, only 5% of DOR* content is bound by Del2. Taken together these data suggest that G-proteins stabilize a high affinity state conformation which does not seem modulated by cholesterol. Moreover, the incorporation of GTP upon agonist binding is modulated by cholesterol content. To explain these results we propose that a fraction of agonist-activated receptor forms requires a cholesterol-rich environment.

The existence of two pools of functional receptors stabilized by a different particular lipid membrane environment could explain that every GPCR activates multiple effectors via coupling to distinct G-proteins. Thus, the current model suggests that isomerisation of receptors upon agonist binding do not only give one active state, but rather at least two active states, each of which interacts with distinct G-proteins triggering different effector pathways [54,55]. Some studies [49] report also that G-proteins target discrete and distinct cell surface microdomains: G_q especially concentrates in caveolae, whereas G_i and G_s concentrate much more in lipid rafts. Indeed, a possible mechanism is that the receptor adopts various conformations in constitutive or active state, each of them requiring a particular lipid environment for specific G-protein interaction.

Likewise, assuming that the pool of DOR* modulated by cholesterol (60%) is related to its localisation in cholesterol-enriched microdomains, we ask whether a pool of receptors could be recruited to rafts. Under the conditions of DRMs isolation, only less than a 30% of the total initial pool of DOR* could be isolated in cholesterol/sphingomyelin-enriched fractions, i.e. half of that expected. To understand these discrepancies, it should be noted that although domains isolated after TX-100 solubilisation contain pre-existing *lo* domains, they do not entirely represent existing domains in their native state [14], and we showed that the raft markers and DOR* proportions recruited in these cholesterol-rich and sphingomyelin-rich fractions depend on detergent/lipid ratios. Interestingly, DRM isolation demonstrated a two-fold increase in DOR* content upon agonist binding, in the low-density cholesterol/sphingomyelin-enriched fraction (LDFp); this can be clearly ascribed to rafts microdomains and our data suggest that this fraction recruited in LDF_P upon Del2 binding might be a G-protein coupled form of the receptor. These findings are consistent with our previous purposes: a pool of constitutively G-protein coupled receptors is in a poor cholesterol environment and need a cholesterol-rich environment upon agonist binding.

5. Conclusion

In light of the significance of the existence of rafts, there are still open questions: (i) what is the driving force for sequestering the receptor into various lipid microdomains? Various factors involved in the sorting of proteins to specific microdomains have been suggested [44]: specific interactions with lipids (cholesterol) may be involved for some proteins [56]. One would also expect that the trans-bilayer pressure of each microdomain can control the conformational equilibrium of proteins [57]. Another issue is hydrophobic matching between the transmembrane domains of the protein and the lipid environment. In this context, to explain our data, we propose that the stabilization of each DOR* form may be achieved via a mechanism of protein sorting. We assume that cholesterol, in proportion to its local concentration, promotes microdomains with distinct thicknesses; the hydrophobic matching principle could be a driving force involved in lipid and protein sorting. Thus, our results suggest that the DOR* structure adapts oneself in each microdomain. The elongated DOR* forms, induced upon Del2 binding [20], require a rearrangement of the lateral distribution of molecules to stabilize these new DOR* conformations. The variation in the total cholesterol concentration modulates these molecular distributions and adaptations, likewise the activity of DOR* forms. We plan to test this hypothesis by investigating the effect of the acyl-chain length of the phospholipids on the function and lateral distribution of the reconstituted DOR*.

Acknowledgements

This study was supported by the CNRS (Centre National de la Recherche Scientifique) and the ARC (Association pour la Recherche contre le Cancer). A.A. was supported by a grant from FSE (Fonds Social Européen).

References

[1] M. Edidin, Lipid microdomains in cell surface membranes, Curr. Opin. Struct. Biol. 7 (1997) 528–532.
[2] K. Simons, D. Toomre, Lipid rafts and signal transduction, Nat. Rev., Mol. Cell. Biol. 1 (2000) 31–39.
[3] A. Becher, R.A. McIlhinney, Consequences of lipid raft association on G-protein-coupled receptor function, Biochem. Soc. Symp. (2005) 151–164.
[4] K. Simons, W.L. Vaz, Model systems, lipid rafts, and cell membranes, Annu. Rev. Biophys. Biomol. Struct. 33 (2004) 269–295.
[5] A. Kusumi, W.K. Subczynski, M. Pasenkiewicz-Gierula, J.S. Hyde, H. Merkle, Spin-label studies on phosphatidylcholine-cholesterol membranes: effects of alkyl chain length and unsaturation in the fluid phase, Biochim. Biophys. Acta 854 (1986) 307–317.
[6] P.F. Almeida, W.L. Vaz, T.E. Thompson, Lateral diffusion in the liquid phases of dimyristoylphosphatidylcholine/cholesterol lipid bilayers: a free volume analysis, Biochemistry 31 (1992) 6739–6747.
[7] M.B. Sankaram, T.E. Thompson, Cholesterol-induced fluid-phase immiscibility in membranes, Proc. Natl. Acad. Sci. U. S. A. 88 (1991) 8686–8690.
[8] X. Xu, R. Bittman, G. Duportail, D. Heissler, C. Vilcheze, E. London, Effect of the structure of natural sterols and sphingolipids on the formation of ordered sphingolipid/sterol domains (rafts). Comparison of cholesterol to plant, fungal, and disease-associated sterols and comparison of sphingomyelin, cerebrosides, and ceramide, J. Biol. Chem. 276 (2001) 33540–33546.
[9] S. Munro, Lipid rafts: elusive or illusive? Cell 115 (2003) 377–388.
[10] M. Edidin, The state of lipid rafts: from model membranes to cells, Annu. Rev. Biophys. Biomol. Struct. 32 (2003) 257–283.
[11] N.M. Hooper, Detergent-insoluble glycosphingolipid/cholesterol-rich membrane domains, lipid rafts and caveolae (review), Mol. Membr. Biol. 16 (1999) 145–156.

[12] J.L. Rigaud, B. Pitard, D. Levy, Reconstitution of membrane proteins into liposomes: application to energy-transducing membrane proteins, Biochim. Biophys. Acta 1231 (1995) 223–246.
[13] S. Schuck, M. Honsho, K. Ekroos, A. Shevchenko, K. Simons, Resistance of cell membranes to different detergents, Proc. Natl. Acad. Sci. U. S. A. 100 (2003) 5795–5800.
[14] A.E. Garner, A. Smith, N.M. Hooper, Visualisation of detergent solubilisation of membranes: implications for the isolation of rafts, Biophys. J. 94 (2008) 1326–1340.
[15] E.B. Babiychuk, A. Draeger, Biochemical characterization of detergent-resistant membranes: a systematic approach, Biochem. J. 397 (2006) 407–416.
[16] S. Moffett, D.A. Brown, M.E. Linder, Lipid-dependent targeting of G proteins into rafts, J. Biol. Chem. 275 (2000) 2191–2198.
[17] B. Chini, M. Parenti, G-protein coupled receptors in lipid rafts and caveolae: how, when and why do they go there? J. Mol. Endocrinol. 32 (2004) 325–338.
[18] Z. Salamon, S. Cowell, E. Varga, H.I. Yamamura, V.J. Hruby, G. Tollin, Plasmon resonance studies of agonist/antagonist binding to the human delta-opioid receptor: new structural insights into receptor–ligand interactions, Biophys. J. 79 (2000) 2463–2474.
[19] I.D. Alves, S.M. Cowell, Z. Salamon, S. Devanathan, G. Tollin, V.J. Hruby, Different structural states of the proteolipid membrane are produced by ligand binding to the human delta-opioid receptor as shown by plasmon-waveguide resonance spectroscopy, Mol. Pharmacol. 65 (2004) 1248–1257.
[20] I.D. Alves, Z. Salamon, V.J. Hruby, G. Tollin, Ligand modulation of lateral segregation of a G-protein-coupled receptor into lipid microdomains in sphingomyelin/phosphatidylcholine solid-supported bilayers, Biochemistry 44 (2005) 9168–9178.
[21] S. Kalipatnapu, A. Chattopadhyay, Membrane organization of the human serotonin (1A) receptor monitored by detergent insolubility using GFP fluorescence, Mol. Membr. Biol. 22 (2005) 539–547.
[22] A. Saulière, G. Gaibelet, C. Millot, S. Mazères, A. Lopez, L. Salomé, Diffusion of the mu opioid receptor at the surface of human neuroblastoma SH-SY5Y cells is restricted to permeable domains, FEBS. Lett. 580 (2006) 5227–5231.
[23] Y. Cheng, W.H. Prusoff, Relationship between the inhibition constant (K1) and the concentration of inhibitor which causes 50 per cent inhibition (I50) of an enzymatic reaction, Biochem. Pharmacol. 22 (1973) 3099–3108.
[24] O.H. Lowry, N.J. Rosebrough, A.L. Farr, R.J. Randall, J. Biol.Chem. 193 (1951) 265–275.
[25] E.G. Bligh, W.J. Dyer, A rapid method of total lipid extraction and purification, Can. J. Med. Sci. 37 (1959) 911–917.
[26] B. Zak, R.C. Dickenman, E.G. White, H. Burnett, P.J. Cherney, Rapid estimation of free and total cholesterol, Am. J. Clin. Pathol. 24 (1954) 1307–1315.
[27] G. Rouser, S. Fkeischer, A. Yamamoto, Two dimensional then layer chromatographic separation of polar lipids and determination of phospholipids by phosphorus analysis of spots, Lipids 5 (1970) 494–496.
[28] H. Bullova, P. Balgavy, Turbidimetric study of unilamellar extruded egg phosphatidylcholine liposomes, Acta Facultatis Pharmaceuticae Universitatis Comenianae Tomus II (2005).
[29] J.R. Lakowicz, Principles of fluorescence spectroscopy, Plenum Press, New-York, 1999.
[30] S. Mazères, V. Schram, J.F. Tocanne, A. Lopez, 7-nitrobenz-2-oxa-1,3-diazole-4-yl-labeled phospholipids in lipid membranes: differences in fluorescence behavior, Biophys. J. 71 (1996) 327–335.
[31] G. Patterson, R.N. Day, D. Piston, Fluorescent protein spectra, J. Cell. Sci. 114 (2001) 837–838.
[32] J.A. Riddick, W.B. Bunger, Organic Solvents. Physical Properties and Methods of Purification, John Wiley and Sons, New-York, 1970.
[33] H.I. Mosberg, R. Hurst, V.J. Hruby, K. Gee, H.I. Yamamura, J.J. Galligan, T.F. Burks, Bis-penicillamine enkephalins possess highly improved specificity toward delta opioid receptors, Proc. Natl. Acad. Sci. U. S. A. 80 (1983) 5871–5874.
[34] A. Misicka, A.W. Lipkowski, L. Fang, R.J. Knapp, P. Davis, T. Kramer, T.F. Burks, H.I. Yamamura, D.B. Carr, V.J. Hruby, Topographical requirements for delta opioid ligands: presence of a carboxyl group in position 4 is not critical for deltorphin high delta receptor affinity and analgesic activity, Biochem. Biophys. Res. Commun. 180 (1991) 1290–1297.
[35] J. Sot, L.A. Bagatolli, F.M. Goni, A. Alonso, Detergent-resistant, ceramide-enriched domains in sphingomyelin/ceramide bilayers, Biophys. J. 90 (2006) 903–914.
[36] M.C. Giocondi, B. Seantier, P. Dosset, P.E. Milhiet, C. Le Grimellec, Characterizing the interactions between GPI-anchored alkaline phosphatases and membrane domains by AFM, Pflugers. Arch. 456 (2008) 179–188.
[37] K. Gaus, M. Rodriguez, K.R. Ruberu, I. Gelissen, T.M. Sloane, L. Kritharides, W. Jessup, Domain-specific lipid distribution in macrophage plasma membranes, J. Lipid Res. 46 (2005) 1526–1538.
[38] L.J. Pike, X. Han, K.N. Chung, R.W. Gross, Lipid rafts are enriched in arachidonic acid and plasmenylethanolamine and their composition is independent of caveolin-1 expression: a quantitative electrospray ionization/mass spectrometric analysis, Biochemistry 41 (2002) 2075–2088.
[39] P. Drevot, C. Langlet, X.J. Guo, A.M. Bernard, O. Colard, J.P. Chauvin, R. Lasserre, H.T. He, TCR signal initiation machinery is pre-assembled and activated in a subset of membrane rafts, EMBO J. 21 (2002) 1899–1908.
[40] W. Drobnik, H. Borsukova, A. Bottcher, A. Pfeiffer, G. Liebisch, G.J. Schutz, H. Schindler, G. Schmitz, Apo AI/ABCA1-dependent and HDL3-mediated lipid efflux from compositionally distinct cholesterol-based microdomains, Traffic 3 (2002) 268–278.
[41] K. Röper, D. Corbei, W.B. Huttner, Retention of prominin in microvilli reveals distinct cholesterol-based lipid micro-domains in the apical plasma membrane, Nat. Cell Biol. 2 (2000) 582–592.
[42] P.F. Lenne, L. Wawrezinieck, F. Conchonaud, O. Wurtz, A. Boned, X.J. Guo, H. Rigneault, H.T. He, D. Marguet, Dynamic molecular confinement in the plasma membrane by microdomains and the cytoskeleton meshwork, EMBO J. 25 (2006) 3245–3256.
[43] J.L. Macdonald, L.J. Pike, A simplified method for the preparation of detergent-free lipid rafts, J. Lipid Res. 46 (2005) 1061–1067.
[44] L.J. Pike, Lipid rafts: heterogeneity on the high seas, Biochem. J. 378 (2004) 281–292.
[45] P. Samama, S. Cotecchia, T. Costa, R.J. Lefkowitz, A mutation-induced activated state of the beta 2-adrenergic receptor. Extending the ternary complex model, J. Biol. Chem. 268 (1993) 4625–4636.
[46] P. Huang, W. Xu, S.I. Yoon, C. Chen, P.L. Chong, L.Y. Liu-Chen, Cholesterol reduction by methyl-beta-cyclodextrin attenuates the delta opioid receptor-mediated signaling in neuronal cells but enhances it in non-neuronal cells, Biochem. Pharmacol. 73 (2007) 534–549.
[47] F. Galbiati, B. Razani, M.P. Lisanti, Emerging themes in lipid rafts and caveolae, Cell 106 (2001) 403–411.
[48] G.P. Eckert, U. Igbavboa, W.E. Muller, W.G. Wood, Lipid rafts of purified mouse brain synaptosomes prepared with or without detergent reveal different lipid and protein domains, Brain Res. 962 (2003) 144–150.
[49] P. Oh, J.E. Schnitzer, Segregation of heterotrimeric G proteins in cell surface microdomains. G(q) binds caveolin to concentrate in caveolae, whereas G(i) and G(s) target lipid rafts by default, Mol. Biol. Cell 12 (2001) 685–698.
[50] J.E. Schnitzer, D.P. McIntosh, A.M. Dvorak, J. Liu, P. Oh, Separation of caveolae from associated microdomains of GPI-anchored proteins, Science 269 (1995) 1435–1439.
[51] A.D. Albert, J.E. Young, P.L. Yeagle, Rhodopsin–cholesterol interactions in bovine rod outer segment disk membranes, Biochim. Biophys. Acta 1285 (1996) 47–55.
[52] B. Lagane, G. Gaibelet, E. Meilhoc, J.M. Masson, L. Cézanne, A. Lopez, Role of sterols in modulating the human mu-opioid receptor function in *Saccharomyces cerevisiae*, J. Biol. Chem. 275 (2000) 33197–33200.
[53] T.J. Pucadyil, A. Chattopadhyay, Role of cholesterol in the function and organization of G-protein coupled receptors, Prog. Lipid Res. 45 (2006) 295–333.
[54] D.M. Perez, J. Hwa, R. Gaivin, M. Mathur, F. Brown, R.M. Graham, Constitutive activation of a single effector pathway: evidence for multiple activation states of a G protein-coupled receptor, Mol. Pharmacol. 49 (1996) 112–122.
[55] T. Kenakin, Agonist–receptor efficacy. II. Agonist trafficking of receptor signals, Trends Pharmacol. Sci. 16 (1995) 232–238.
[56] K. Burger, G. Gimpl, F. Fahrenholz, Regulation of receptor function by cholesterol, Cell. Mol. Life Sci. 57 (2000) 1577–1592.
[57] F. Abe, H. Iida, Pressure-induced differential regulation of the two tryptophan permeases Tat1 and Tat2 by ubiquitin ligase Rsp5 and its binding proteins, Bul1 and Bul2, Mol. Cell. Biol. 23 (2003) 7566–7584.